LIMNOLOGY and OCEANOGRAPHY

ASLO

Limnol. Oceanogr. 9999, 2021, 1–8

doi: 10.1002/lno.11913

Resilience of phytoplankton dynamics to trophic cascades and nutrient enrichment

Stephen R. Carpenter ,[1*] **Babak M.S. Arani,**[2] **Egbert H. Van Nes,**[2] **Marten Scheffer,**[2] **Michael L. Pace**[3]

[1]Center for Limnology, University of Wisconsin, Madison, Wisconsin
[2]Aquatic Ecology and Water Quality Management, Wageningen University, Wageningen, The Netherlands
[3]Department of Environmental Sciences, University of Virginia, Charlottesville, Virginia

Abstract

Resilience was compared for alternate states of phytoplankton pigment concentration in two multiyear whole-lake experiments designed to shift the manipulated ecosystem between alternate states. Mean exit time, the average time between threshold crossings, was calculated from automated measurements every 5 min during summer stratification. Alternate states were clearly identified, and equilibria showed narrow variation in bootstrap analysis of uncertainty. Mean exit times ranged from 13 to 290 h. In the reference ecosystem, Paul Lake, mean exit time of the low-pigment state was about 100 h longer than mean exit time of the high-pigment state. In the manipulated ecosystem, Peter Lake, mean exit time of the high-pigment state exceeded that of the low-pigment state by 30 h in the cascade experiment. In the enrichment experiment mean exit time of the low-pigment state was longer than that of the high-pigment state by about 100 h. Mean exit time is a useful measure of resilience for stochastic ecosystems where high-frequency measurements are made by consistent methods over the full range of ecosystem states.

Lake ecosystems provide diverse examples of complex dynamics, including multiple stable states and critical transitions among them (Scheffer 1998, 2009). These include alternate states of phytoplankton biomass resulting from either trophic cascades or nutrient enrichment (Carpenter 2003).

Holling (Holling 1973) recognized that ecosystems exhibit multiple states and occasionally shift among them. Holling introduced *resilience* as "the persistence of relationships within a system" and "a measure of the ability of these systems to absorb changes of state variables, driving variables, and parameters, and still persist." He distinguished resilience from *stability*, "the ability of a system to return to an equilibrium state after a temporary disturbance." Unlike stability which is a local measure that treats perturbations as isolated events, resilience accounts for perturbations of large amplitudes and the ongoing tempo of sequential disturbances. A section titled "The Random World" (pp. 13–15 of Holling 1973) discusses the role of random fluctuations in resilience, including examples from lake eutrophication, food webs, and fisheries. Holling's ideas of resilience imply probabilities of persistence of an ecosystem state or identity in a stochastic environment. However, most research has focused on deterministic aspects of resilience and few quantitative studies have addressed resilience in a stochastic framework.

Arani et al. (2021) proposed "exit time" as a stochastic measure of resilience. Exit time, a stochastic variable, is the average time until a shift between states of a stochastic system is first observed. The mean exit time, or the median, can serve as a resilience measure. A familiar example is half-life of a radioisotope. Decay from the radioactive state to the daughter state is a stochastic process of single atoms. Its half-life is the median exit time, or time until half of the radioactive atoms have decayed. In global change science, Kleinen et al. (2003) mentioned exit time from Atlantic Meridional Overturning Circulation (AMOC, the state of the ocean that brings a mild climate to Western Europe) as a measure of the expected time available for policy action to maintain resilience of Europe's climate. Arani et al. (2021) present empirical methods for measuring exit time from ecosystem states using time series data. We apply that method here to assess resilience of experimental lakes to trophic cascades and nutrient enrichment.

In 2008, we began a series of experiments designed to gradually shift lake ecosystems between alternate states. Our goal was to evaluate dynamic indicators of resilience based on

*Correspondence: steve.carpenter@wisc.edu

Additional Supporting Information may be found in the online version of this article.

Author Contribution Statement: The whole-lake experiments were designed and conducted by S.R.C. and M.L.P.; the method for exit time was developed by B.M.S.A., E.H.V.N., and M.S.; the R programs were written by S.R.C. and B.M.S.A.; data analysis and graphics were done by S.R.C.; and all authors contributed to the writing.

statistical changes in time series as the lake shifted from one state to another (Carpenter et al. 2011; Scheffer et al. 2015; Pace et al. 2017; Wilkinson et al. 2018). Because these studies measured lake ecosystem variables frequently during both states of the ecosystem and the transition, the data are suitable for estimating exit time. Here, we determine mean exit times for two different manipulations that induced alternate states and provided high-frequency time series needed to assess exit time as a quantitative measure of resilience as described by Holling (1973).

Methods

Peter and Paul Lakes

Paul and Peter lakes are paired lakes in Gogebic County, Michigan, USA (46°250 N, 89°500 W). Since 1951 the lakes have been used for whole-lake experiments with Paul as the reference lake and Peter as the manipulated lake (Elser et al. 1986). Since 1984 the lakes have been used for a series of experiments on trophic cascades, allochthony measured by ^{13}C addition, and eutrophication by nutrient enrichment (Carpenter and Pace 2018).

Trophic cascade experiment

At the start of the trophic cascade experiment, Peter Lake's food web was dominated by planktivorous minnows. In 2008 and 2009, small numbers of adult largemouth bass (*Micropterus salmoides* L.) were gradually added to Peter Lake (Carpenter et al. 2011). A large year class of bass resulted in 2010. Increasingly with bass additions, minnows sought refuge in shallow water and the surrounding bog (Cline et al. 2014). The decline of minnow numbers in offshore waters was followed by expansion of large-bodied grazing zooplankton (Pace et al. 2013) and decline in chlorophyll concentration (Carpenter et al. 2011). Paul Lake's food web was dominated by largemouth bass throughout the experiment (Carpenter et al. 2011).

Nutrient enrichment experiment

Nutrients in the form of inorganic phosphorus and nitrogen were added to enrich Peter Lake in 2013, 2014, and 2015. Nutrients were added daily over the summer season for the first 2 yrs and only until early warning signals were obtained in the third year (Pace et al. 2017; Wilkinson et al. 2018). Phytoplankton responded to the additions of nutrients but bloom timing and magnitude varied considerably among years (Wilkinson et al. 2018). Paul Lake, which drains into Peter Lake, did not receive added nutrients and served as an unmanipulated reference ecosystem.

High-frequency pigment measurements

We used automated pigment measurements during summer stratification to estimate mean exit times. Data were recorded every 5 min.

During the cascade experiment, each lake was monitored with two Yellow Springs Instruments multiparameter sondes (model 6600-V2-4) equipped with optical chlorophyll *a* (Chl *a*) sensors (model 6025) deployed at a depth of 0.7 m at a central station (Batt et al. 2013). Chl *a* is reported in μg/L. We did not use phycocyanin sensors in this study because cyanobacteria were at low concentrations throughout and did not reflect the dynamics of the phytoplankton community.

During the enrichment experiment each lake was monitored with a Hydrolab DS5X sonde including a sensor for phycocyanin fluorescence (model 007291) deployed at a depth of 0.75 m (Pace et al. 2017). Chlorophyll sensors in this study were not responsive to phytoplankton blooms unlike direct manual measurements of extracted chlorophyll (S.I.). Unknown processes likely related to the presence of large cyanobacterial filaments resulted in low detection of chlorophyll—a phenomena observed by others (Gregor and Maršálek 2004). Phycocyanin fluorescence and extracted chlorophyll had similar dynamics consistent with limited microscopic counts indicating blooms were dominated by cyanobacteria (Wilkinson et al. 2018). Phycocyanin is reported in relative fluorescence units (RFU). Direct laboratory measurements of phycocyanin concentration (μg/L) were linearly related to RFU (Pace et al. 2017).

Estimation of mean exit time

Mean exit time was estimated by the following steps: (1) Standardize the pigment time series (Arani et al. 2021) (S.I. *Dynamic Linear Models*); (2) Test the Markov hypothesis for standardized time series by the Langevin method (S.I. *Assessment of the Markov Property and Stationarity*). (3) Test the stationarity of the standardized time series by the augmented Dickey–Fuller (ADF) test (S.I. *Assessment of the Markov Property and Stationarity*). (4) Using the standardized time series, estimate the deterministic and stochastic components of a Langevin model (system reconstruction); (5) Calculate mean exit time for the ecosystem states of interest.

The in situ sensors detected chlorophyll for the cascade experiment and phycocyanin for the enrichment experiment. We used standardized levels of pigment fluorescence (S.I. *Dynamic Linear Models* and Figs. S-1, S-2, S-3, and S-4) as indicators of pigment concentration for both experiments. For the standardized levels reported here, the ADF test rejected the null hypothesis of non-stationarity ($p < 0.01$ for each lake in each experiment) and data exhibited the Markov property (S.I. *Assessment of Markov Property and Stationarity*).

Langevin analysis

Exit time develops from terms of the Langevin Eq. 1 as summarized in several works (Siegert et al. 1998; Siegert and Friedrich 2001; Rinn et al. 2016; Tabar 2019). A detailed description of exit time analysis is presented by Arani et al. (2021). We present an abbreviated explanation here. A complete worked example (Peter Lake in the enrichment experiment) is provided as R scripts: https://github.com/SRCarpen/ExitTime_BinMethod_PeterLakeExample

The time series of standardized levels b_t/s_t were used as state variables (x_t) to estimate the drift-diffusion model known as the Langevin equation (Carpenter and Brock 2011; Rinn et al. 2016; Tabar 2019)

$$dx = D_1(x)dt + \sqrt{2D_2(x)}\,dW \tag{1}$$

The implementation in R is based on Rinn et al. (2016) and the Matlab code of Arani et al. (2021). $D_1(x)$ is the deterministic core of the dynamics called the "drift" in stochastic dynamic modeling. Its roots $D_1(x) = 0$ are the equilibria. $D_2(x)$, called "diffusion" in stochastic modeling, is a deterministic function that represents the intensity of the noise as a function of x. The noise source is dW where W stands for the Wiener process, and thus dW represents Gaussian white noise. The fitted drift and diffusion functions are used below in calculations of effective potential, the stationary distribution, and mean exit time.

In this paper, diffusion functions are plotted using the definition

$$D_2(x) = \frac{1}{2}\sigma^2(x) \tag{2}$$

Thus $\sigma(x) = \sqrt{2D_2(x)}$, and this conversion allows drift and diffusion to be compared in the same units, pigment standardized level/time.

Potential and effective potential

Stability of dynamic systems can be illustrated by potential curves, or "ball and cup" diagrams that show stable points as valleys and unstable points as hilltops. For deterministic systems, the potential curve $P(x)$ is the integral

$$U(x) = \int^{x} D_1(z)dz \tag{3}$$

where z is a dummy variable and the integral is computed over the relevant range of x.

The potential $U(x)$ does not account for the noise of the system. Studies of resilience should account for the possibility that random events may change the shape of the potentials (Horsthemke and Lefever 1984). Effects of noise are included in the effective potential, $U_E(x)$ (Arani et al. 2021) and we use his function here

$$U_E(x) = -\int^{x} \frac{D_1(z)}{D_2(z)}dz + \log(D_2(x)) \tag{4}$$

Exit time

For both lakes in both experiments, the drift function D_1 describes a curve with two stable equilibria separated by an unstable equilibrium (main text Figs. 1–4). The expected exit times from each stable basin can be estimated by solving the backward Fokker–Planck equation with appropriate boundary conditions for each basin:

$$D_1(x)\frac{dT}{dx} + D_2(x)\frac{d^2T}{dx^2} = -1 \tag{5}$$

The solution of this equation, given the boundary conditions, is mean exit time $T(x)$ if the starting state of the system is x. For each basin, we use an absorbing boundary at the middle unstable equilibrium where small random disturbance can cause a shift between basins. For the outer boundaries (left boundary of the left basin, right boundary of the right basin) we use a reflecting

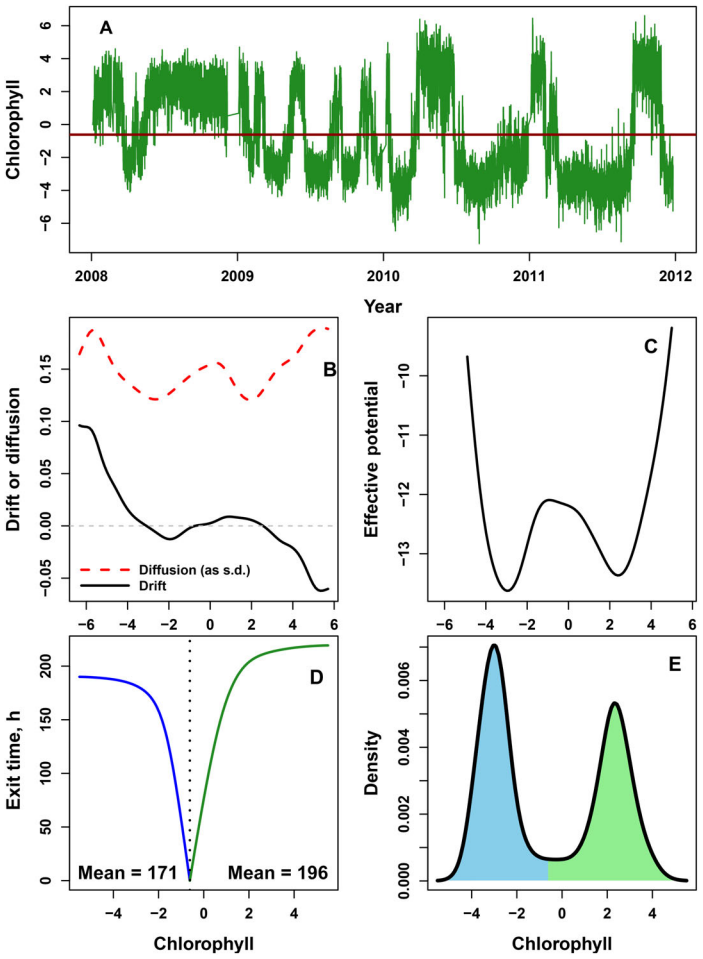

Fig. 1. Resilience analysis of manipulated Peter Lake during the Cascade experiment. (**A**) Chlorophyll (standardized level) vs. year during the experiment. Solid horizontal line denotes the unstable threshold. (**B**) Drift (black) and diffusion (red) functions vs. chlorophyll standardized level. (**C**) Effective potential vs. chlorophyll standardized level. (**D**) Exit time (h) vs. chlorophyll standardized level, with probability-weighted means, for the two stable basins. Vertical dotted line is the threshold between the basins. (**E**) Stationary probability density vs. chlorophyll standardized level. Shading denotes the low-chlorophyll (blue) and high-chlorophyll (green) basins.

boundary to indicate that no shift occurs. If the boundary is absorbing, $T(x) = 0$ at the boundary, i.e., the exit time is 0 at the unstable edge between basins. If the boundary is reflecting, the derivative $\frac{dT}{dx} = 0$ at the boundary, i.e., there is no change in $T(x)$ at the reflecting boundary. For calculations, we chose the left reflecting boundary slightly above the lower limit of the data and the right reflecting boundary slightly below the upper limit of the data.

We solved the boundary-value problem (5) with the bvpSolve() package in R using function bvptwp() (Mazzia et al. 2014). An R script to illustrate the method using a simple ecological model is found at https://github.com/SRCarpen/Exit_Time_R

Solving for $T(x)$ yields mean exit time as a function of x. It is useful to have a single representative value of exit time for an entire basin. We estimated a basin-wide mean exit time for the full width of each basin as the probability-weighted mean of $T(x)$ with probabilities taken from the normalized stationary density of the Fokker–Planck equation which is computed from D_1 and D_2 (Horsthemke and Lefever 1984; Arani et al. 2021). For example, the mean of $T(x)$ is $p(x)T(x)$ where $p(x)$ is the stationary probability that sums to 1 over all values of x. We integrated the stationary density using the hcubature() function of the cubature() package in R (https://bnaras.github.io/cubature/).

Uncertainty of exit time

To assess uncertainty of exit time, we first bootstrapped the autoregressions by randomizing the errors (ε_t, Eq. S-1a) with replacement and adding them to the predicted y_t to generate pseudodata (Efron and Tibshirani 1993). The pseudodata series were fit to the Dynamic Linear Model (Eqs. S-1) and standardized levels were used to estimate drift and diffusion (Eq. 2), exit times (Eq. 5) and the stationary probability distribution. One hundred bootstrap cycles were run, and the distribution of exit times was corrected for bias (Efron and Tibshirani 1993).

Results

Alternate states and resilience: Cascade experiment

Chlorophyll concentration time series during summer stratification for manipulated Peter Lake and reference Paul Lake were measured during the summer stratified seasons of 2008–2011 (Figs. S1, S2).

Standardized levels of chlorophyll (Fig. 1A) in Peter Lake were used to estimate components of a Langevin model (Fig. 1A). Diffusion (variability) is larger than the deterministic rate of change (drift) (Fig. 1B). We plotted sigma (Eq. 2) so that both components have the same units.

Chlorophyll dynamics in Peter Lake are dominated by noise. Nonetheless the drift function indicates three equilibria (three crossings of the line y = 0). The left and right equilibria are stable, because a small increase in chlorophyll decreases the rate of change causing chlorophyll to decrease toward the equilibrium point, and a small decrease in chlorophyll increases the rate of change, restoring chlorophyll toward the equilibrium point. The center equilibrium is unstable because small changes of chlorophyll in either direction cause chlorophyll to shift away from the center equilibrium. Thus, the center equilibrium is a threshold separating two alternate stable equilibria. The alternate equilibria represent the minnow dominated (higher chlorophyll) and bass dominated (lower chlorophyll) states. The effective potential (Eq. 4) shows two distinct stability basins (Fig. 1C).

Exit time as a function of the initial value of chlorophyll is zero at the unstable equilibrium, because a small perturbation of chlorophyll at that point can shift the ecosystem in either

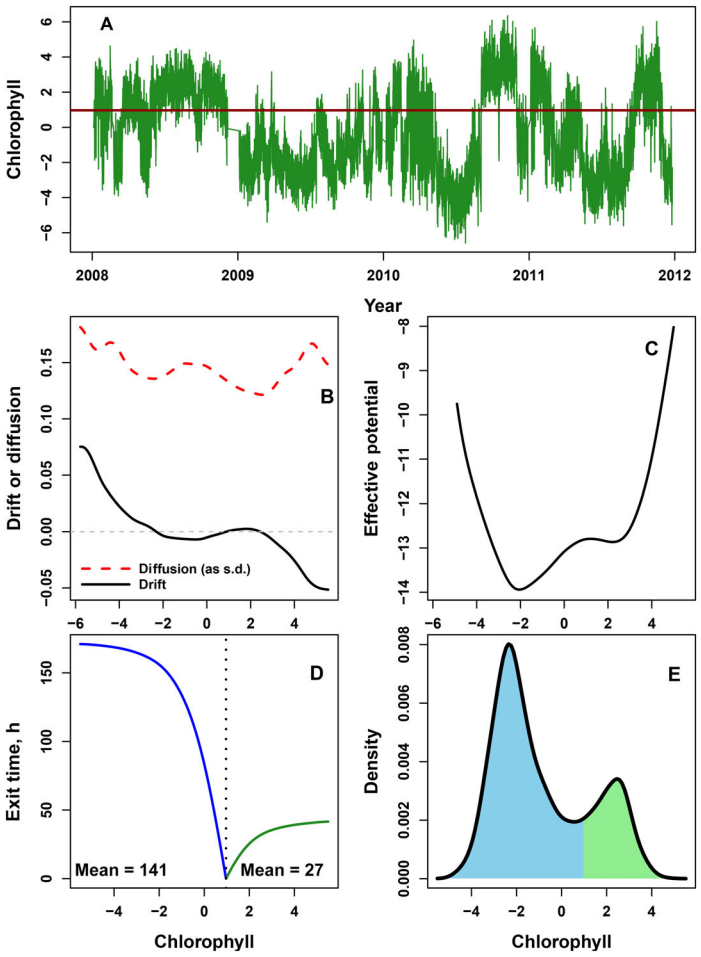

Fig. 2. Resilience analysis of Paul Lake, reference ecosystem for the Cascade experiment. (**A**) Chlorophyll (standardized level) vs. year during the experiment. Solid horizontal line denotes the unstable threshold. (**B**) Drift (black) and diffusion (red) functions vs. chlorophyll standardized level. (**C**) Effective potential vs. chlorophyll standardized level. (**D**) Exit time (h) vs. chlorophyll standardized level, with probability-weighted means, for the two stable basins. Vertical dotted line is the threshold between the basins. (**E**) Stationary probability density vs. chlorophyll standardized level. Shading denotes the low-chlorophyll (blue) and high-chlorophyll (green) basins.

direction (Fig. 1D). Exit times rise as chlorophyll moves either direction from the unstable equilibrium.

To obtain an average exit time over each basin, we calculate the weighted averages where the weights are the normalized stationary densities for starting values of chlorophyll (Fig. 1D, E). The two states of the ecosystem are apparent in the stationary probability distribution. The mean exit times of the low and high chlorophyll basins are 171 h and 196 h, respectively.

Fluctuations of chlorophyll in Paul Lake represent the baseline variability of an unmanipulated ecosystem (Fig. 2A). Although the diffusion is much larger than the drift, alternate equilibria are discernible (Fig. 2B). Mean exit times of low and high chlorophyll equilibria are 141 and 27 h, respectively (Fig. 2D,E).

Alternate states and resilience: Nutrient enrichment experiment

Phycocyanin RFU were highly variable in manipulated Peter Lake (Fig. 3) and reference Paul Lake during the enrichment experiment (Fig. 4).

Standardized levels of phycocyanin in Peter Lake suggest shifts from low- to high-pigment levels during each year (Fig. 3A). Diffusion (as sigma (Eq. 2), in the same units as drift) was notably larger than drift (Fig. 3B). The effective potential

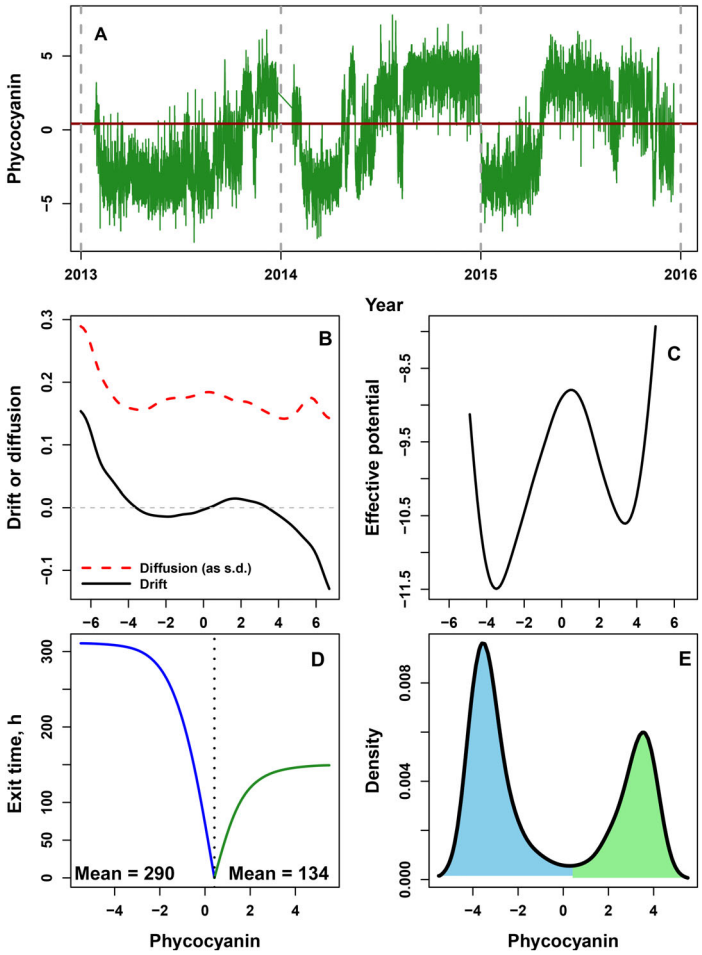

Fig. 3. Resilience analysis of enriched Peter Lake during the enrichment experiment. (**A**) Phycocyanin (standardized level) vs. year during the experiment. Solid horizontal line denotes the unstable equilibrium. (**B**) Drift (black) and diffusion (red) functions vs. phycocyanin standardized level. (**C**) Effective potential vs. phycocyanin standardized level. (**D**) Exit time (h) vs. phycocyanin standardized level, with probability-weighted means, for the two stable basins. Vertical dotted line is the threshold between the basins. (**E**) Stationary probability density vs. phycocyanin standardized level. Shading denotes the low-phycocyanin (blue) and high-phycocyanin (green) basins.

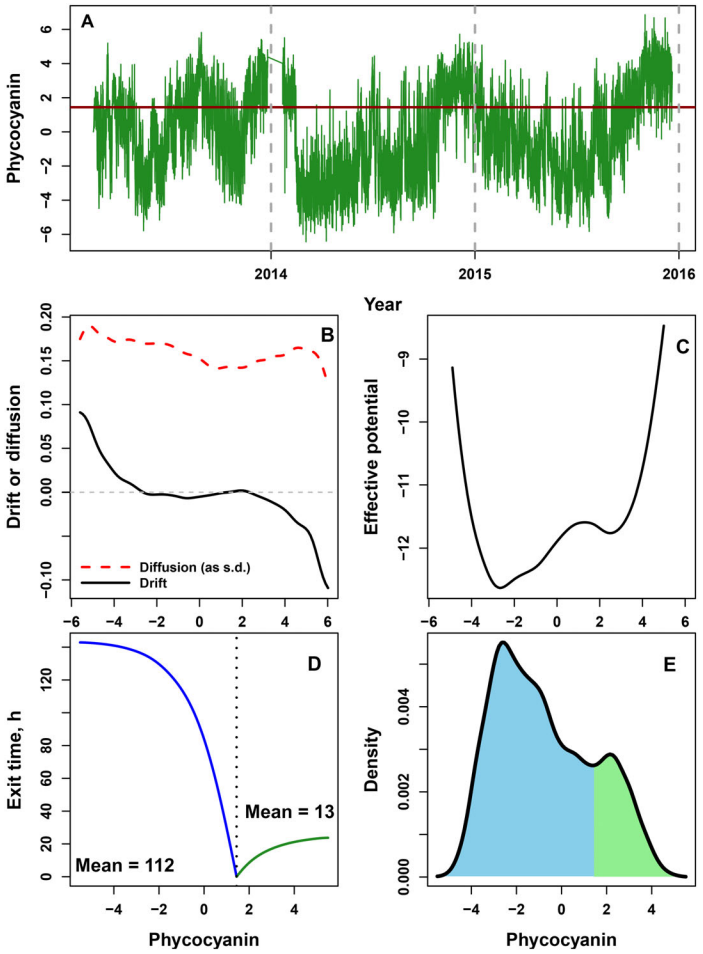

Fig. 4. Resilience analysis of Paul Lake during the enrichment experiment. (**A**) Phycocyanin (standardized level) vs. year during the experiment. Solid line denotes the unstable equilibrium. (**B**) Drift (black) and diffusion (red) functions vs. phycocyanin standardized level. (**C**) Effective potential vs. phycocyanin standardized level. (**D**) Exit time (h) vs. phycocyanin standardized level, with probability-weighted means, for the two stable basins. Vertical dotted line is the threshold between the basins. (**E**) Stationary probability density vs. phycocyanin standardized level. Shading denotes the low-phycocyanin (blue) and high-phycocyanin (green) basins.

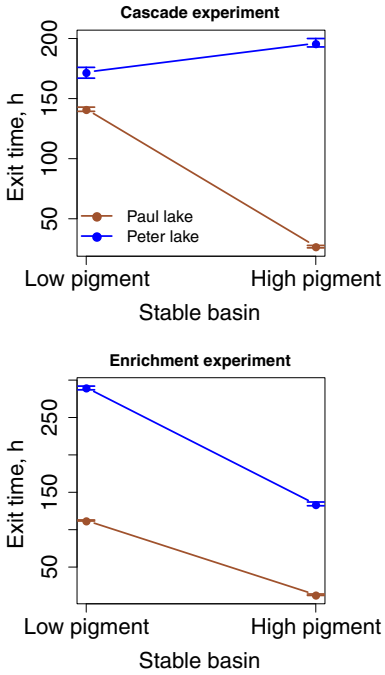

Fig. 5. Exit time for low- and high-pigment stable basins for both lakes during the cascade and enrichment experiments. Error bars show the interquartile range (25th to 75th percentile) and circle shows the median (50th percentile) of 100 bootstrap samples (S.I.).

showed two stable basins, but the high-phycocyanin basin appears shallower than the low-phycocyanin basin (Fig. 3C). Exit times are zero at the unstable transition point between the basins, and rise to the left and right of the transition point (Fig. 3D). The two basins of attraction are evident in the stationary probability density (Fig. 3E). The probability-weighted exit times are 290 h for the low-phycocyanin basin and 134 h for the high-phycocyanin basin.

Paul Lake also exhibited seasonal fluctuations in standardized level of phycocyanin (Fig. 4A). Diffusion was much larger than the drift (Fig. 4B) but nonetheless alternate states are evident in the effective potential (Fig. 4C) and density (Fig. 4E). Exit times are 112 h for the low-pigment basin and 13 h for the high-pigment basin (Fig. 4D).

Validation of the models

For each dataset the one-step predictions of the fitted Langevin equations compared to data had a lower negative log likelihood than a hypothetical model with constant drift (S.I. *Model Validation*). To visualize the goodness of fit we compared one-step conditional probabilities predicted by the Langevin equations with the observed one-step changes of the data for selected initial points quantiles in each lake in each experiment (S.I. *Model Validation* and Fig. S5). Predicted distributions closely matched observed distributions.

Uncertainty of exit time estimates

Distributions of the deterministic equilibria (zeroes of the drift function) were estimated by bootstrapping (S.I. Figs. S6, S7). For Peter Lake, each bootstrapped pseudo-dataset, 100 for each experiment, had three equilibria, two stable equilibria separated by an unstable threshold. The variability of estimated equilibria is relatively narrow and equilibria are well-separated on the pigment axes (Fig. S6). For Paul Lake equilibria were distinct and variability was modest (Fig. S7).

Distributions of mean exit time from 100 bootstrap cycles were computed for both stable basins in both experiments (S.I. Figs. S8, S9). Exit time includes the stochasticity of the dynamics (diffusion). Patterns of the distributions were different among experiments, lakes, and stability basins.

In manipulated Peter Lake, exit times were longer than in unmanipulated Paul Lake based on interquartile ranges (Fig. 5). Exit time from the low-pigment basin was longer than exit time from the high-pigment basin in Paul Lake. In Peter Lake for the cascade experiment the high-pigment equilibrium had longer exit time than the low-pigment equilibrium. In the enrichment experiment, this pattern was reversed with shorter exit time in the high-pigment equilibrium.

Discussion

The long-term condition of both lakes is the low-pigment state. In Peter Lake the manipulations caused short-term excursions into the high-pigment state, but by different mechanisms. In the cascade experiment, intervals of high chlorophyll were caused by fluctuations in grazing associated with movement of planktivorous fishes between littoral and pelagic habitats (Pace et al. 2013; Cline et al. 2014). In the nutrient enrichment experiment, intervals of high phycocyanin were associated with accumulation of phosphorus and nitrogen in phytoplankton (Wilkinson et al. 2018). When manipulations ended, the ecosystem returned to the low-pigment pre-manipulation state. For both experiments, phase-randomized surrogate time series did not have alternate states, suggesting that alternate states were not likely to be detected by chance (S.I. *Could Alternate States be Detected by Chance?*).

In Paul Lake, fluctuations of pigment concentrations are due to the routine dynamics of phytoplankton in a variable physical–chemical environment, interacting with grazers in an ecosystem that was not manipulated. Note that Paul Lake lies upstream of Peter Lake, was sampled using a separate boat, and was not contaminated with added nutrients. Chlorophyll fluctuations in Paul Lake show occasional brief peaks in the epilimnion (Fig. S2) as seen in previous studies (Carpenter and Kitchell 1993; Carpenter et al. 2001). Weekly phytoplankton counts in Paul Lake from 1984–1997 showed both absence and occasional peaks of Cyanobacteria that are consistent with the patterns we observed in high-frequency phycocyanin data (Cottingham et al. 1998). These fluctuations could have appeared as alternate states in our analysis.

We were surprised to see alternate states in the high-frequency pigment data from Paul Lake. The experiments were designed initially to test dynamic indicators of resilience. In Peter Lake, several dynamic indicators provided early warnings of loss of resilience but no indications of declining resilience were detected in Paul Lake (Carpenter et al. 2011; Batt et al. 2013; Pace et al. 2013, 2017; Cline et al. 2014; Wilkinson et al. 2018).

We considered the possibility that cyclic fluctuations in irradiance, temperature or other variables could appear to be alternate states in sensor data. During each experiment in each lake, daily samples were taken, returned to the laboratory, and analyzed by fluorometry to measure Chl *a* concentration (Carpenter et al. 2011; Pace et al. 2017). Drift functions of the Langevin Eq. 1 for daily chlorophyll time series show alternate states for the manipulated lake, Peter Lake, but not for the reference Paul Lake (Fig. S-10 and S.I. *Alternate States in Daily Chlorophyll Time Series*). However, the diffusion component is relatively large, consistent with the sensor data. Because of the daily time step and small sample size (about 120 daily samples per year vs. 288 sensor samples per day, or about 34,560 sensor samples per year in each lake), we did not attempt to estimate exit time from the daily data. Patterns in the daily data are consistent with the alternate states we detected in Peter Lake but ambiguous with regard to the alternate states we detected in Paul Lake. Further research using high-frequency pigment measurements in a wider variety of aquatic environments is needed to improve understanding of alternate states of phytoplankton and the response of stochastic indicators such as exit time.

An exit event occurs when the pigment line crosses the unstable equilibrium that separates the two basins (Figs. 1A, 2A, 3A, 4A). Most of the intervals between exit events are short, and some quick events are hidden by the width of the plotted lines. Thus, the mean exit times range from about 1 to 10 d due to the dominance of short events (Fig. 5). These rather short mean exit times are another indication of the high variability of the time series.

To be useful an indicator of stochastic resilience should be repeatable, comparable among ecosystems, responsive to changes in resilience, and have low-to-moderate uncertainty for real-world time series. In addition, for our method the time series to be analyzed should meet the assumptions of the Langevin method. For these sensors and these lakes, the standardized levels analyzed here meet these conditions. Different data standardizations may be appropriate for different ecosystems or sensors.

In summary, resilience of phytoplankton biomass (as measured here by their pigments) in lake ecosystems may depend on slowly-changing variables such as watershed sources of nutrients and colored Dissolved Organic Carbon, sediment release of nutrients, grazer dynamics, and apex predators. Gradual trends of such variables reduce resilience and increase the likelihood that random events can cause a regime shift (Holling 1973; Scheffer et al. 2001). Our experiments simulated gradual forcing of Peter Lake by trophic cascades or nutrients. Pigment concentration, especially in sensor optical measurements, is highly variable and this variance strongly affects resilience measured using exit time and likely other stochastic indicators. The temporal fluctuations of chlorophyll are large enough that thresholds are crossed every few days when measured by high-frequency sensors during multiyear whole-lake experiments. We suspect that a decades-long perspective of high-frequency measurements could reveal much longer exit times for past states of Peter Lake, consistent with patterns seen in paleolimnological records (Leavitt et al. 1989). Nonetheless we have shown a pathway for comparative resilience studies of lake ecosystems using resilience measures that are consistent with Holling's (Holling 1973) emphasis of random fluctuations as a key element of resilience. The challenge is to build long-term highly-resolved datasets needed to measure stochastic variates that may provide a quantitative indicators for comparing resilience among aquatic ecosystems.

Data availability statement

Data used here are downloadable from: (1) Carpenter, S., M. Pace, J. Cole, R. Batt, C. Buelo, and J. Kurzweil. 2018. Cascade Project at North Temperate Lakes LTER High Frequency Sonde Data from Food Web Resilience Experiment 2008–2011 ver 1. Environmental Data Initiative. https://doi.org/10.6073/pasta/5a8c6398661fad0bc8f1f5119b1150d6. (2) Pace, M., J. Cole, and S. Carpenter. 2020. Cascade project at North Temperate Lakes LTER—High Frequency Data for Whole Lake Nutrient Additions 2013–2015 ver 2. Environmental Data Initiative. https://doi.org/10.6073/pasta/cbe19041db41e720d84970f43156c042

References

Arani, B. M. S., S. R. Carpenter, L. Lahti, E. H. Van Nes, and M. Scheffer. 2021. Exit time as a measure of ecological resilience. Science **372** eaay4895. doi:10.1126/science.aay4895

Batt, R. D., S. R. Carpenter, J. J. Cole, M. L. Pace, and R. A. Johnson. 2013. Changes in ecosystem resilience detected in automated measures of ecosystem metabolism during a whole-lake manipulation. Proc. Natl. Acad. Sci. **110** 17398–403. doi:10.1073/pnas.1316721110

Carpenter, S. R. 2003. Regime shifts in lake ecosystems: Pattern and variation. Ecology Institute, ISSN 0932-2205.

Carpenter, S. R., and W. A. Brock. 2011. Early warnings of unknown nonlinear shifts: a nonparametric approach. Ecology **92** 2196–201. doi:10.1890/11-0716.1

Carpenter, S. R., and J. F. Kitchell [eds.]. 1993. Trophic cascades in lakes. Cambridge Univ. Press. ISBN 0 521 43145 X.

Carpenter, S. R., and M. L. Pace. 2018. Synthesis of a 33-yr series of whole-lake experiments: Effects of nutrients, grazers, and precipitation-driven water color on chlorophyll. Limnol. Oceanogr. Lett. **3** 419–27. doi:10.1002/lol2.10094

Carpenter, S. R., and G. D. Peterson. 2019. C. S. 'Buzz' Holling, 6 December 1930–2016 August 2019. Nat. Sustain. **2** 997–8. doi:10.1038/s41893-019-0425-9

Carpenter, S. R., and others. 2001. Trophic cascades, nutrients and lake productivity: whole-lake experiments. Ecol. Monogr. **71** 163–86. doi:10.2307/2657215

Carpenter, S. R., and others. 2011. Early warnings of regime shifts: a whole-ecosystem experiment. Science **332** 1079–82. doi:10.1126/science.1203672

Cline, T. J., and others. 2014. Early warnings of regime shifts: evaluation of spatial indicators from a whole-ecosystem experiment. Ecosphere **5** 1–13. doi:10.1890/ES13-00398.1

Cottingham, K. L., S. R. Carpenter, and A. L. S. Amand. 1998. Responses of epilimnetic phytoplankton to experimental nutrient enrichment in three small seepage lakes. J. Plankton Res. **20** 1889–914. doi:10.1093/plankt/20.10.1889

Efron, B., and R. J. Tibshirani. 1993. An introduction to the bootstrap. Chapman and Hall. ISBN 0-412-042331-2.

Elser, M. M., J. J. Elser, and S. R. Carpenter. 1986. Paul and Peter Lakes: a liming experiment revisited. Am. Midl. Nat. **116** 282–95. doi:10.2307/2425736

Gregor, J., and B. Maršálek. 2004. Freshwater phytoplankton quantification by chlorophyll *a*: a comparative study of in vitro, in vivo and in situ methods. Water Res. **38** 517–22. doi:10.1016/j.watres.2003.10.033

Holling, C. S. 1973. Resilience and stability of ecological systems. Annu. Rev. Ecol. Syst. **4** 1–23. doi:10.1146/annurev.es.04.110173.000245

Horsthemke, W., and R. Lefever. 1984. Noise-induced transitions: theory and applications in physics, chemistry and biology. Springer-Verlag. ISBN 0-387-11359-2.

Kleinen, T., H. Held, and G. Petschel-Held. 2003. The potential role of spectral properties in detecting thresholds in the Earth system: application to the thermohaline circulation. Ocean Dyn. **53** 53–63. doi:10.1007/s10236-002-0023-6

Leavitt, P. R., S. R. Carpenter, and J. F. Kitchell. 1989. Whole-lake experiments: the annual record of fossil pigments and zooplankton. Limnol. Oceanogr. **34** 700–17. doi:10.4319/lo.1989.34.4.0700

Mazzia, F., J. Cash, and K. Soetart. 2014. Solving boundary value problems in the open source software R: Package bvpSolve. Opusc. Math. **34** 387–403. doi:10.7494/OpMath.2014.34.2.38

Pace, M. L., S. R. Carpenter, R. A. Johnson, and J. T. Kurzweil. 2013. Zooplankton provide early warnings of a regime shift in a whole-lake manipulation. Limnol. Oceanogr. **58** 525–32. doi:10.4319/lo.2013.58.2.0525

Pace, M. L., and others. 2017. Reversal of a cyanobacterial bloom in response to early warnings. Proc. Natl. Acad. Sci. **114** 352–7. doi:10.1073/pnas.1612424114

Rinn, P., P. G. Lind, M. Wachter, and J. Peinke. 2016. The Langevin approach: an R package for modeling Markov processes. J. Open Res Softw. **4** e34. doi:10.5334/jors.123

Scheffer, M. 1998. Ecology of shallow lakes. Springer-Verlag. ISBN 978-1-4020-3154-0.

Scheffer, M. 2009. Critical transitions in nature and society. Princeton Univ. Press. ISBN 978-0691-12204-5.

Scheffer, M., S. Carpenter, J. A. Foley, C. Folke, and B. Walker. 2001. Catastrophic shifts in ecosystems. Nature **413** 591–6. doi:10.1038/35098000

Scheffer, M., S. R. Carpenter, V. Dakos, and E. H. V. Nes. 2015. Generic indicators of ecological resilience: inferring the chance of a critical transition. Annu. Rev. Ecol. Evol. Syst. **46** 145–67. doi:10.1146/annurev-ecolsys-112414-054242

Siegert, S., and R. Friedrich. 2001. Modeling of nonlinear Lévy processes by data analysis. Phys. Rev. E **64** 041107. doi:10.1103/PhysRevE.64.041107

Siegert, S., R. Friedrich, and J. Peinke. 1998. Analysis of data sets of stochastic systems. Phys. Lette. A **243** 275–80. doi:10.1016/S0375-9601(98)00283-7

Tabar, M. R. R. 2019. Analysis and data-based reconstruction of complex nonlinear dynamical systems. Springer Nature. ISBN 978-3-030-18472-8.

Wilkinson, G. M., and others. 2018. Early warning signals precede cyanobacterial blooms in multiple whole-lake experiments. Ecol. Monogr. **88** 188–203. doi:10.1002/ecm.1286

Acknowledgments

This paper is dedicated to the memory of Buzz Holling, creative innovator and practitioner of resilience thinking (Carpenter and Peterson 2019). We thank Jonathan J. Cole, James R. Hodgson, and James F. Kitchell for their co-leadership of the whole lake experiments. We are grateful for the contributions of many talented graduate students, postdoctoral trainees, technicians, and undergraduates to the field work. Information management was assisted by the North Temperate Lakes Long-Term Ecological Research program (NSF cooperative agreement DEB-1440297). The University of Notre Dame Environmental Research Center and Trout Lake Station of the University of Wisconsin-Madison provided material support to this research. NSF supported all of the whole-lake experiments through a series of grants. This synthesis was supported by OPUS grants DEB-1455461 and DEB-1456151 to S.R.C. and M.L.P.

Conflict of Interest

None declared.

Submitted 08 February 2021
Revised 13 May 2021
Accepted 28 July 2021

Associate editor: John Melack

SUPPORTING INFORMATION

for

Resilience of Chlorophyll Dynamics to Trophic Cascades and Nutrient Enrichment

Stephen R. Carpenter*[1], Babak M.S. Arani[2], Egbert H. Van Nes[2], Marten Scheffer[2], Michael L. Pace[3]

[1] Center for Limnology, University of Wisconsin, Madison, WI 53706 U.S.A.

[2] Aquatic Ecology and Water Quality Management, Wageningen University, P.O. Box 47, 6700 AA Wageningen, The Netherlands

[3] Department of Environmental Sciences, University of Virginia, Charlottesville, Virginia 22904 U.S.A.

*Correspondence: Steve.Carpenter@wisc.edu

Contents

Dynamic Linear Models

Dynamic linear models are forecasting models updated sequentially from observations by Bayes' formula (West and Harrison 1989). We applied dynamic linear models or DLMs to high-frequency time series from each experiment to standardize the data prior to Langevin analysis. The time varying-models separate the pigment fluctuations into components corresponding to time-varying level, autocorrelated change, errors of each model component, and observation error (Carpenter et al. 2020; Pole et al. 1994; West and Harrison 1989).

In the DLM for a time-varying autoregression, the intercept b_t and autocorrelation coefficients ϕ_t vary over time, according to independent random walks. For a lag-1 autoregressive process, the data or observation equation is

$$y_{t+1} = b_t + \phi_t y_t + \varepsilon_t \qquad \text{[S-1a]}$$

where y is the observed time series of pigment concentrations, b_t is the time series of the intercept or level parameter, ϕ_t is the time series of the autoregressive parameter, and ε_t is the time series of observation errors. The evolution of parameters over time follows the system equations, one for each parameter

$$b_t = b_{t-1} + \omega_{b,t-1} \qquad \text{[S-1b]}$$

$$\phi_t = \phi_{t-1} + \omega_{\phi,t-1} \qquad \text{[S-1c]}$$

Where $\omega_{b,t-1}$ is the time series of process errors in the level b_t, and $\omega_{\varphi,t-1}$ is the time series of process errors in the autoregression coefficient ϕ. The observation errors and the two process errors are Normal processes independent of each other and over time. By choosing prior distributions for initial values, the full model was estimated sequentially from the data by Bayesian updating (West and Harrison 1989).

Time series of b_t, ϕ_t, their time-varying standard errors s_{bt} and $s_{\phi,t}$, one-step predictions $\tilde{y}_t$ and the observation standard error $s_{\varepsilon,t}$ result from fits of [S1] to the time series x_t. We used the AR(1) model because it had lower AIC than AR(2) or AR(3) models. Equations [S-1] were estimated using the Bayesian updating algorithm in Table 3.2 of Pole et al. (1994). A sample R script is included as Step1 of the worked example posted on https://github.com/SRCarpen/ExitTime_BinMethod_PeterLakeExample

The time series b_t tracks changes in the level of the data and its standard error is $s_{b,t}$ the time-varying error of the level. The standardized intercept $b_t/s_{b,t}$ combines the time-varying level of pigment concentration scaled by its time-varying noise. We used time series of the standardized intercept, or level, $b_t/s_{b,t}$ as the index of time-varying pigment concentration for subsequent analyses. Simulations show that the standardized level correctly identifies alternate states when they are present, and does not suggest alternate states if they are absent (Box S1).

Box S1. Simulation results for a model with one stable equilibrium and a model with alternate states. Each figure shows a simulated time series of 100,000 steps, the standardized level from a DLM fit to the data, and drift and diffusion curves estimated from the standardized level.

The 1-root model represents dynamics of a conservative solute, such as chloride, in a lake. Dynamics follow

$$dx = (a - bx)dt + c\,dW \qquad [B\text{-}1]$$

where input a = 5, loss coefficient b = 1, and the standard deviation of environmental noise c = 1. There is a single stable equilibrium at a/b. The model was solved by the Euler-Maruyama method. The resulting time series and the standardized level have one equilibrium (Fig. B-1).

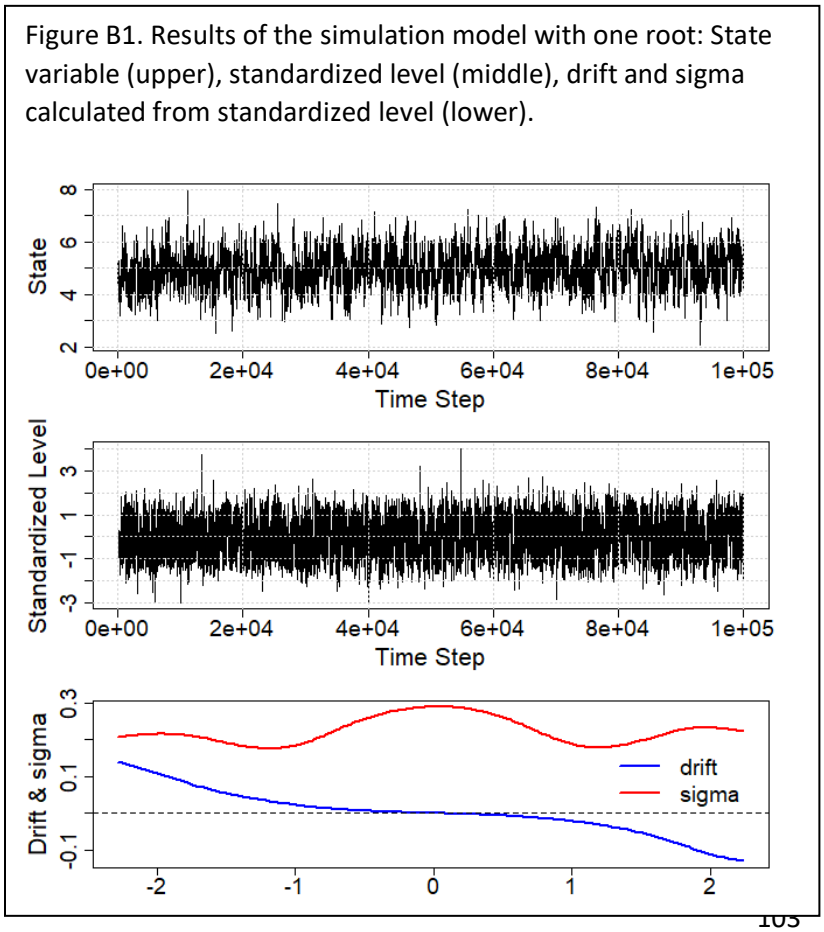

Figure B1. Results of the simulation model with one root: State variable (upper), standardized level (middle), drift and sigma calculated from standardized level (lower).

The model from May (1977) of an exploited population was discretized following Ives and Dakos (Ives and Dakos 2012) as

$$x1 = x0 \exp(f(x0) + Z0 - s^2/2) \quad [B2]$$

$$f(x) = rx(1 - (x/K)) - ax^q/(x^q + h^q)) \quad [B3]$$

with intrinsic growth rate r = 1, carrying capacity K = 10, curvature of the functional response q = 2, maximum loss rate a = 2.2, predation half-saturation h = 1, normally-distributed environmental noise Z0, and standard deviation of the noise s = 0.4. The resulting time series has 3 equilibria, as does the standardized level time series (Figure B2).

Figure B-2. Results of simulating the model with multiple states: State variable (upper), standardized level (middle), drift and sigma calculated from standardized level (lower).

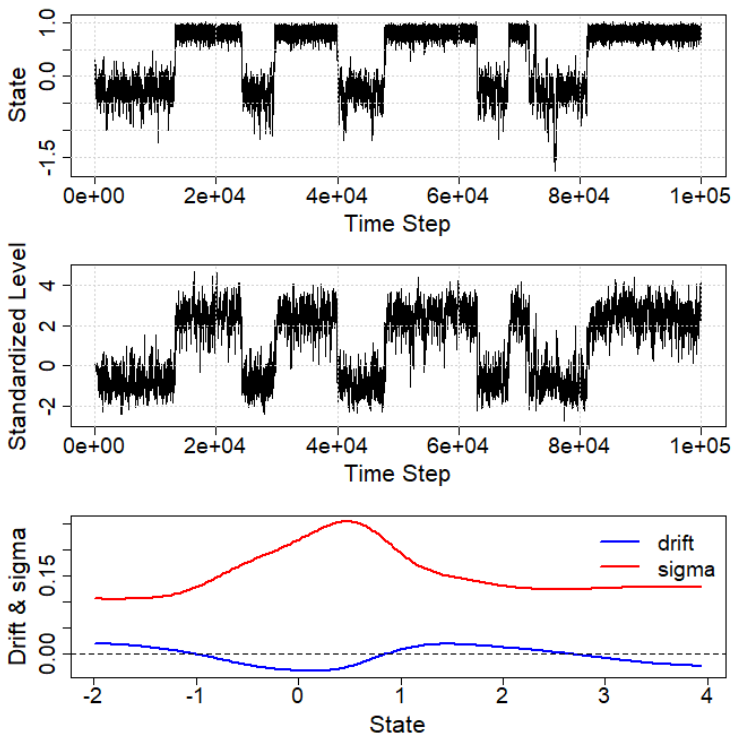

END BOX S1 ----------

Results of dynamic linear models for the manipulated ecosystem, Peter Lake, and reference ecosystem, Paul Lake, in both the Cascade and Enrichment experiments are presented in Figures S1 – S4. Chlorophyll in Peter Lake shows great variability from point to point but nonetheless broad fluctuations are discernible (Fig.S-1A). The time series of the level, b_t, reflects the broad patterns of chlorophyll but also some outliers (Fig. S-1B). The time series of standard error of the level, $s_{b,t}$ shows that some of the outliers have high error (Fig. S-1C). The standardized level, or ratio of level to its standard error $b_t/s_{b,t}$ retains the broad pattern of the chlorophyll time series (Fig. S-1D). Point-to-point variability is large, as seen in the chlorophyll data, and appears consistent throughout the time series.

The same sequence of steps is presented for Paul Lake in the Cascade experiment (Fig. S-2) and both lakes in the Enrichment experiment, Peter (Fig. S-3) and Paul (Fig. S-4). Standardized levels were used for subsequent estimates of exit time.

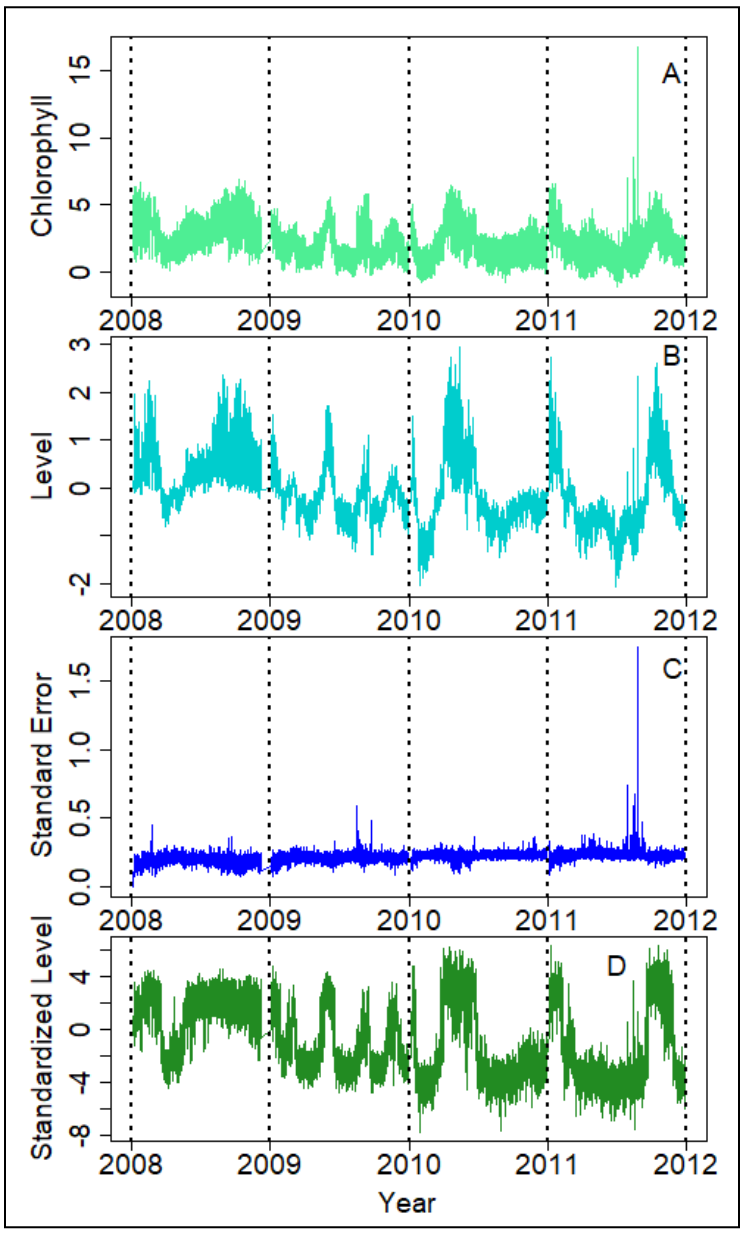

Figure S-1. Cascade experiment: (A) chlorophyll a (µg L^{-1}) measured every 5 minutes in Peter Lake during the summer stratification periods of 2008-2011; (B) Level b_t (intercept of time-varying autoregression) (µg L^{-1}); (C) standard error of level $s_{b,t}$ (µg L^{-1}); (D) standardized level (b_t / $s_{b,t}$), dimensionless).

Figure S-2. Paul Lake, reference ecosystem for the cascade experiment: (A) chlorophyll a (µg L^{-1}) measured every 5 minutes during the summer stratification periods of 2008-2011; (B) Level b_t (intercept of time-varying autoregression) (µg L^{-1}); (C) standard error of level $s_{b,t}$ (µg L^{-1}); (D) standardized level (b_t / $s_{b,t}$., dimensionless).

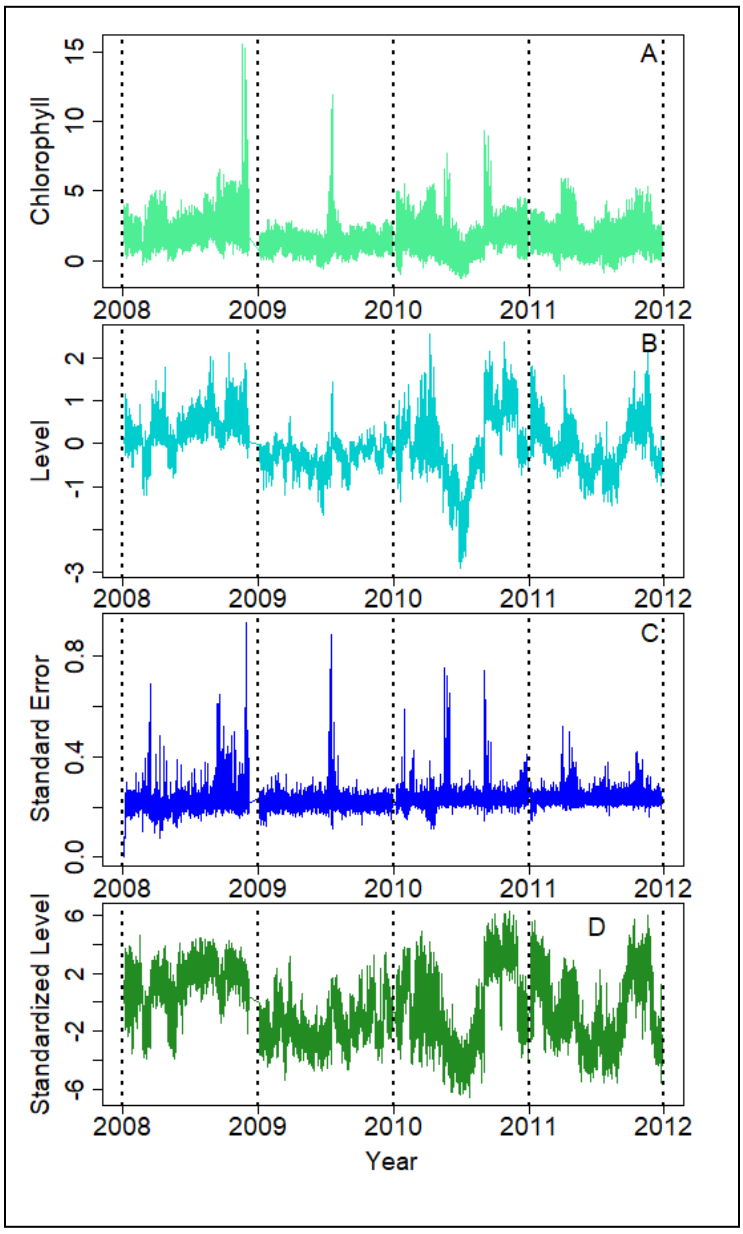

Figure S-3. Enrichment experiment results in Peter Lake: (A) phycocyanin (RFU) measured every 5 minutes in Peter Lake during the summer stratification periods of 2013-2015; (B) Level b_t (intercept of time-varying autoregression) (RFU); (C) standard error of level $s_{b,t}$ (RFU); (D) standardized level (b_t / $s_{b,t}$, dimensionless).

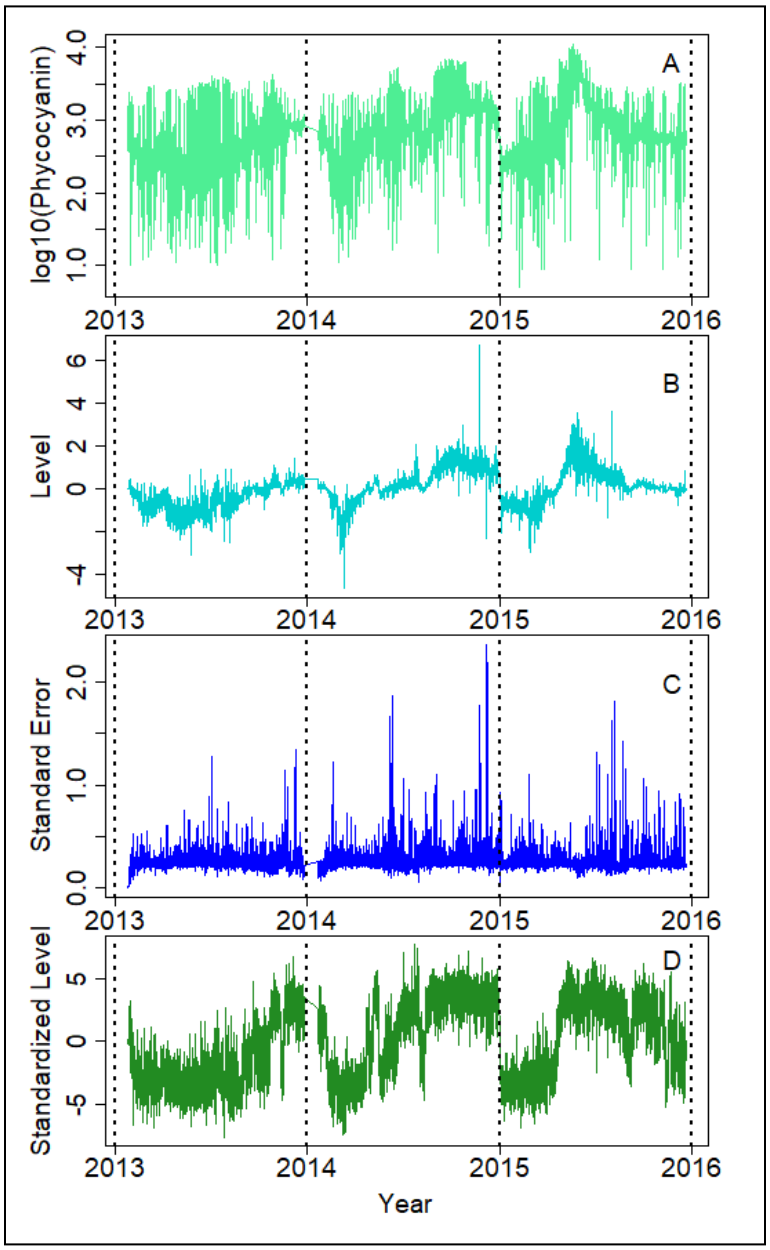

Figure S-4. Paul Lake, reference lake for the enrichment experiment: (A) phycocyanin (RFU) measured every 5 minutes during the summer stratification periods of 2013-2015; (B) Level b_t (intercept of time-varying autoregression) (RFU); (C) standard error of level $s_{b.t}$ (RFU); (D) standardized level (b_t / $s_{b,t}$, dimensionless).

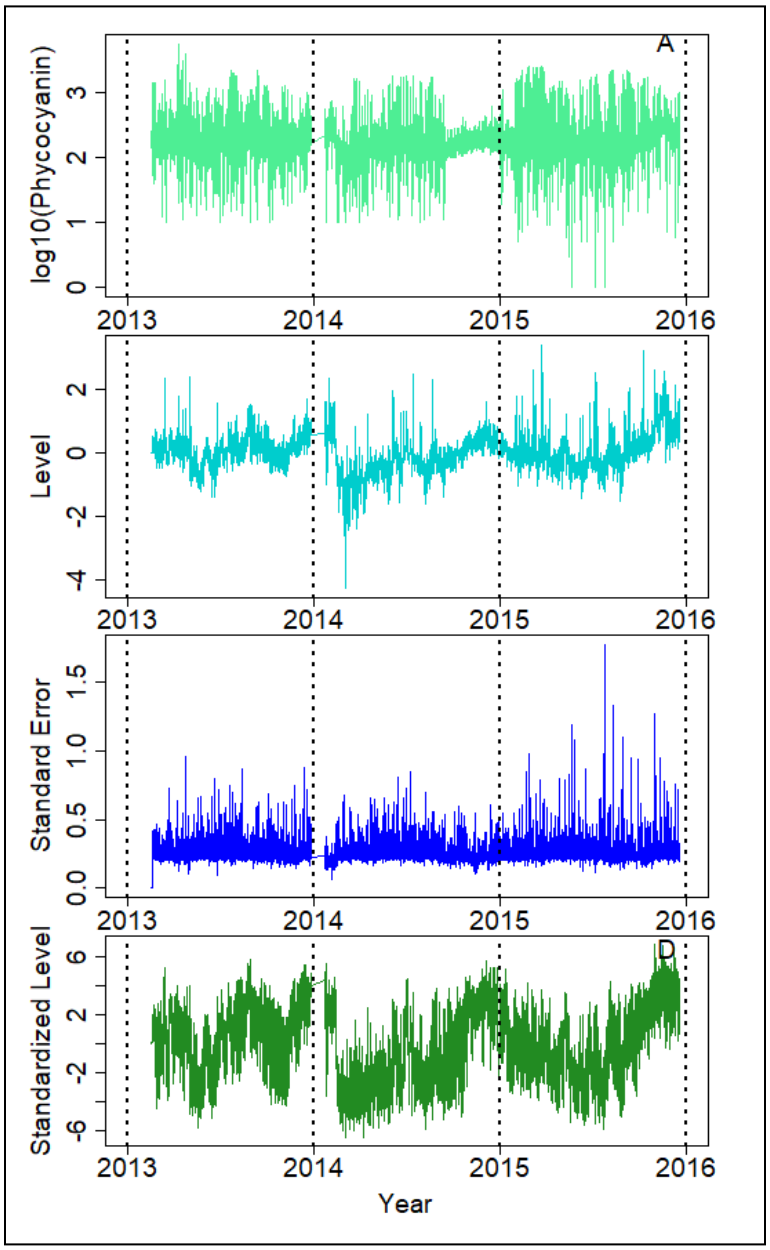

Assessment of the Markov Property and Stationarity

The Langevin approach requires time series with frequent observations and long enough duration to include state transitions (Arani et al. 2021). The dynamics should be represented by the first two moments (i.e. D4 < D2) (Arani et al. 2021; Friedrich et al. 2011). The standardized levels analyzed in this paper met these assumptions.

We assessed stationarity of the data using the augmented Dickey-Fuller (ADF) test (adf.test() in the tseries() library of R) (https://cran.r-project.org/web/packages/tseries/). The null hypothesis of the ADF is that the data are non-stationary. For both lakes in both experiments this hypothesis was rejected ($p < 0.01$). We infer that the data are approximately stationary as expected for Langevin analysis.

In addition the input data for the Langevin analysis should have the Markov property, i.e. each observation depends only on the previous observation and be stationary, i.e. the statistical properties are approximately constant over time (Arani et al. 2021). We tested the Markov hypothesis for each time series of standard level using the Box-Ljung and Rank tests in the R library spgs() available at https://rdrr.io/cran/spgs/man/spgs-package.html. In all cases the Markov property could not be rejected ($p > 0.01$).

As a further test of the Markov property we calculated the so-called 'Markov-Einstein time (ME) scale' using the Chapman-Kolmogorov equation (Arani et al. 2021; Tabar 2019). The ME time scale is determined as a time lag where a χ^2 distance (equation 16.12 of Tabar 2019) is minimal between $p(x_3, t_3|x_1, t_1)$ calculated directly from data versus from the Chapman-Kolmogorov equation. Note that data are Markov if the ME time scale equals one. For our time series the ME time scale is 3 to 6 steps (Figure S5). Although our data are near-Markov we still follow the Langevin approach since it is safer to do so rather than trying to follow more advanced reconstruction schemes designed to account for systems driven by colored noise (Hassanibesheli et al. 2020).

Figure S5. Chi-square distance between the data and the Chapman-Kolmogorov equation versus time lag for Peter Lake in the (A) Cascade and (B) Enrichment experiments, and for Paul Lake in the (C) Cascade and (D) Enrichment experiments

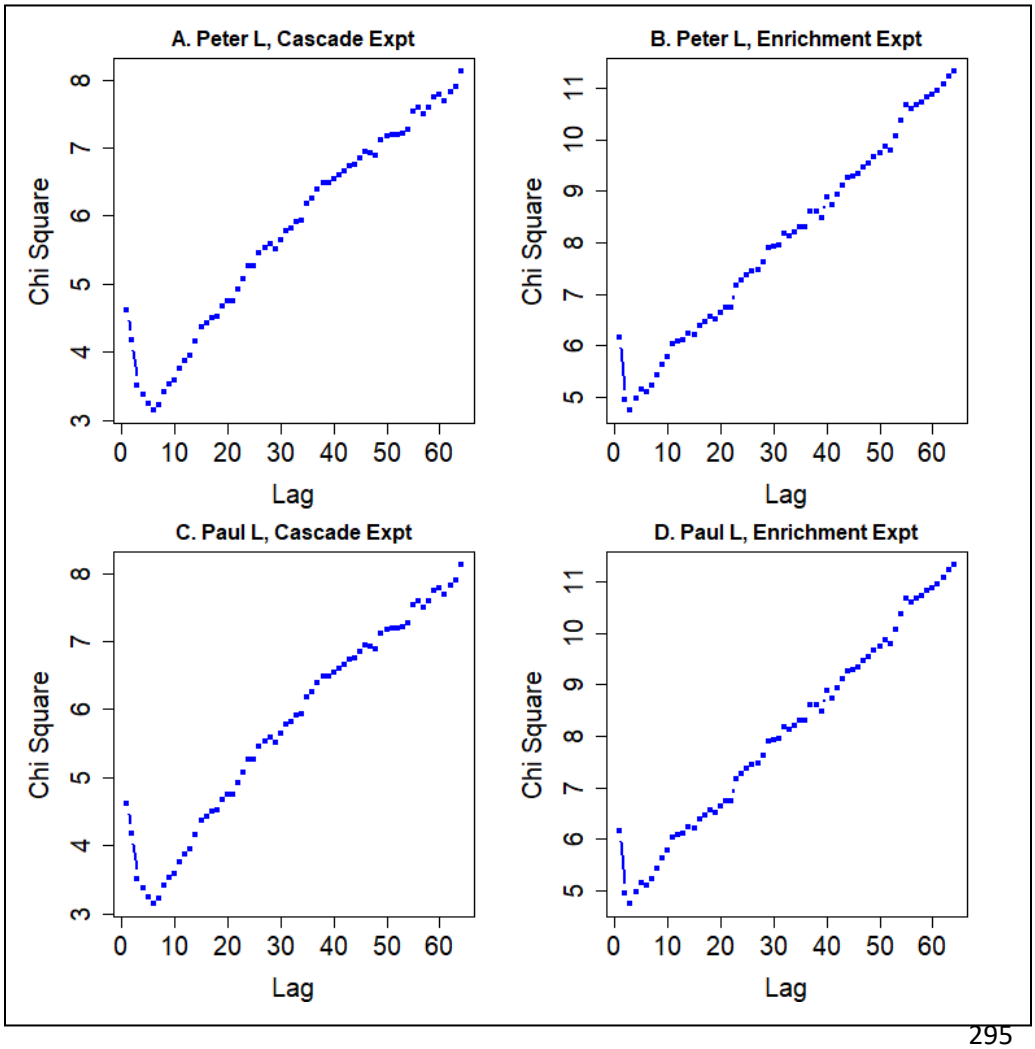

As further illustration that our data conform to the Markov property we compared the data to Chapman-Kolmogorov equation (Fig. S6). A stochastic process x_k sampled at times t_k is said to be Markovian if

$$p(x_k, t_k | x_{k-1}, t_{k-1}, \ldots, x_1, t_1) = p(x_k, t_k | x_{k-1}, t_{k-1}) \qquad [S2]$$

This equation means that the process at any time depends on its previous state only and has no dependency to the remaining past states. There are several ways to assess the Markov property (Tabar 2019). We compared the data to the Chapman-Kolmogorov (CK) equation

$$p(x_3, t_3 | x_1, t_1) = \int p(x_3, t_3 | x_2, t_2)\, p(x_2, t_2 | x_1, t_1)\, dx_2 \qquad [S3]$$

which is valid for all Markov processes. The conditional probability $p(x_3, t_3 | x_1, t_1)$ is calculated in two ways: directly by the data and by the right side of CK equation via two smaller steps at all

intermediate times t_2 ($t_1 < t_2 < t_3$) (Figure S5). This process is suitable because the standardized level time series are approximately stationary (Tabar 2019). The data closely adhere to the Chapman-Kolmogorov equation indicating consistency with the Markov property.

Figure S6. Validation of the Chapman Kolmogorov (CK) equation for a time lag of 1, i.e., the time scale of data, where a close match is observed between $P(x_3|x_1)$ being calculated directly by data (black) and by the right side of eq S3, showing that all datasets are a good approximation of the Markov property. In $P(x_3|x_1)$, x_1 is the initial state which is treated a bin-wise manner so that each peak in the figures represent a particular value of x_1.

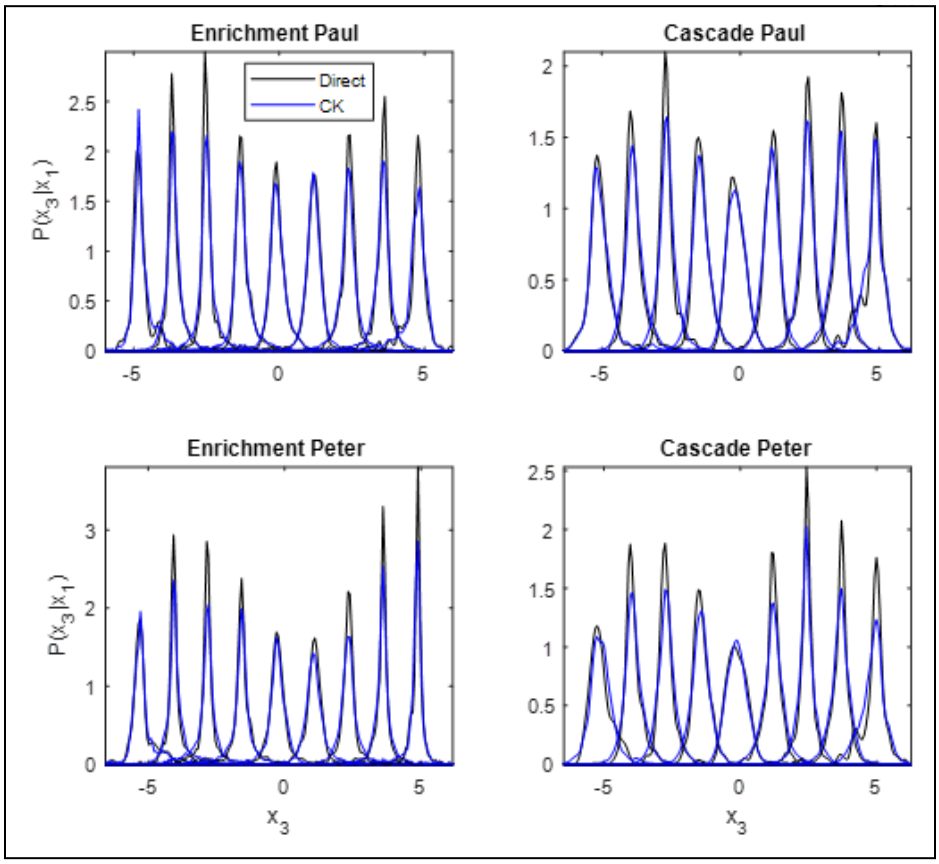

Model Validation

For each lake in each experiment we compared the observed Langevin model to a hypothetical model with constant drift (the mean of the observed drift) using the negative log likelihoods calculated from the one-step model predictions and observations. In all cases the differences in negative log likelihood (observed model – constant drift model) were negative, indicating a better for the observed model. Differences in negative log likelihood for Peter Lake were -17.55 in the Cascade experiment and -6.8 in the Enrichment experiment. In Paul Lake the differences in negative log likelihood were -5.3 in the Cascade experiment and -0.5 in the Enrichment experiment.

To illustrate the correspondence of predictions to observations, we compared the one-step-ahead predicted distributions p(x(t+1)|x(t)) from the Langevin equation with the observed one-step

ahead dynamics of the pigments. Here x(t) is the standardized level of pigment at one point in time. Comparisons were made for each lake in each experiment at 9 quantiles of the frequency distribution of pigment standardized levels.

For the data, we found the corresponding bin for each quartile and then found all pigment values x(t) within this bin. For each x(t) we also found the corresponding observation in the next time step, x(t+1). From these we calculated the distribution of next time step points x(t+1), which is the observed density of next time step points x(t+1) conditioned on the current time step points x(t), i.e., P(x_{t+1}|x_{t}). Using the model, we calculated P(x_{t+1}|x_{t}) from the Langevin equation with terms estimated from the data.

Comparison of the observed and modeled one-step distributions are presented in Fig. S-7. Predicted distributions tightly overlapped with observed distributions.

Figure S-7. Observed (black) and predicted (blue) one-step probability distributions for 9 quartiles of pigment standard level in each lake in each experiment.

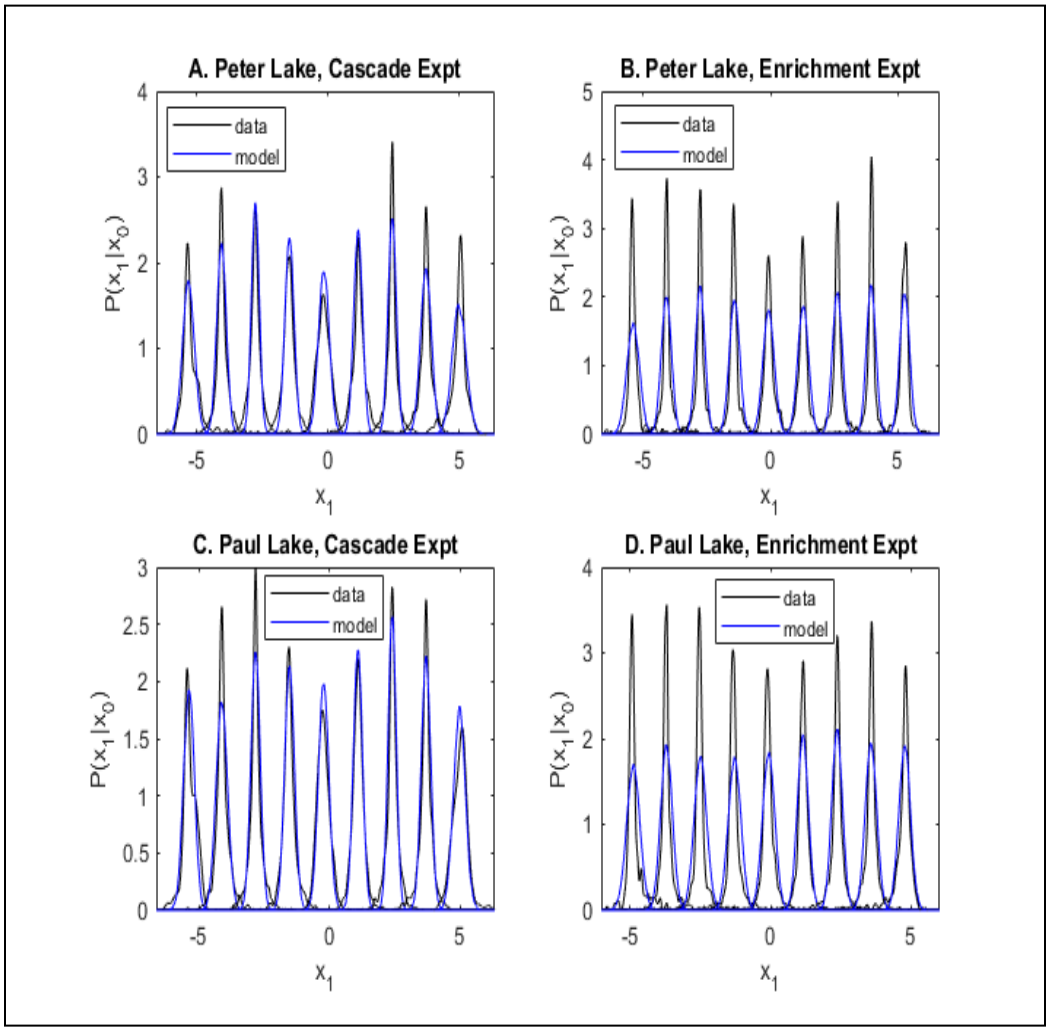

372 ***Bootstrapped Uncertainties for the Equilibria***

373 Figure S-6. Bootstrap estimates of uncertainties for the 3 equilibria in Peter Lake for the Cascade
374 experiment (top row, standardized level of chlorophyll *a*) and enrichment experiment (bottom
375 row, standardized level of phycocyanin). Vertical dashed lines show equilibria of the original
376 data.

377

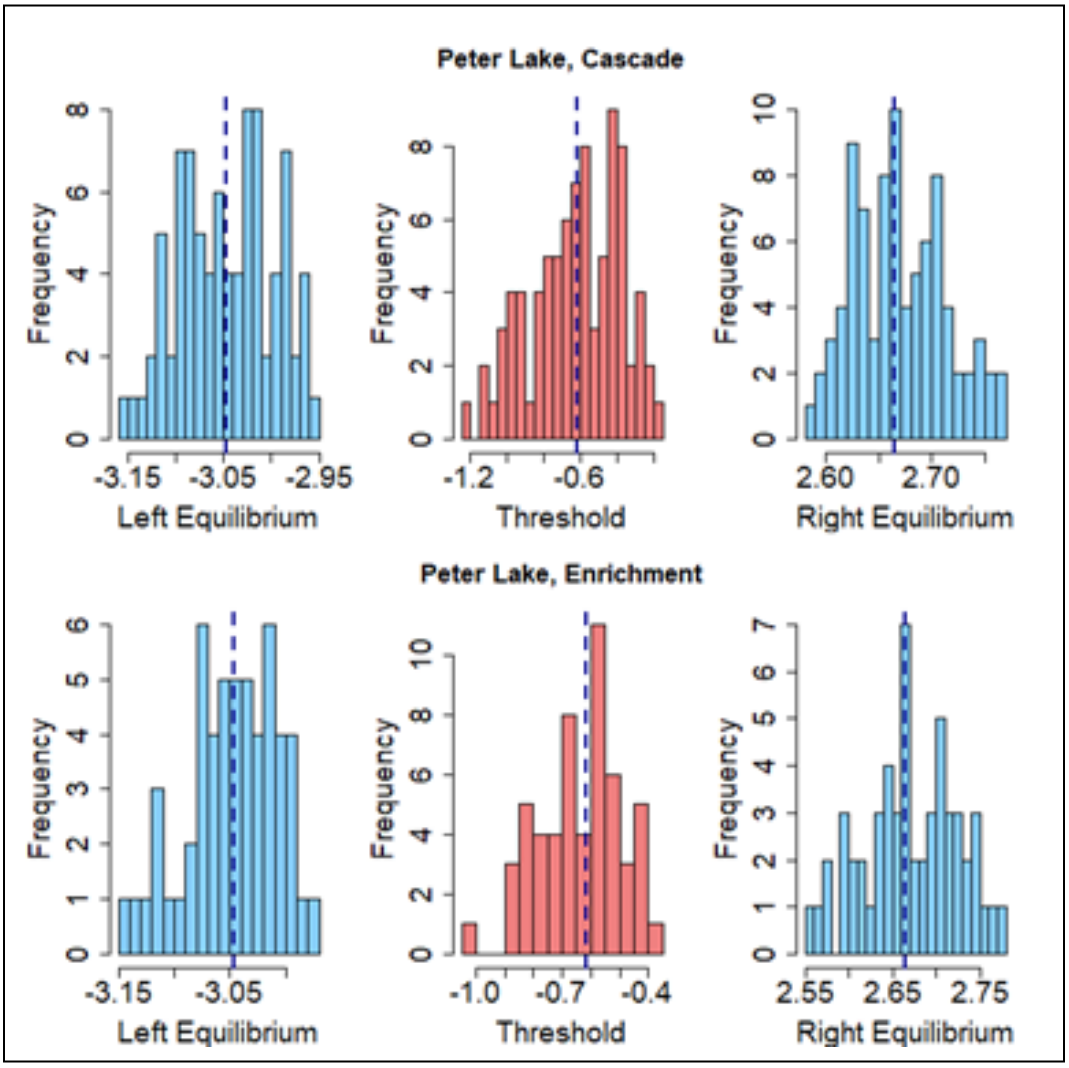

Figure S-7. Bootstrap estimates of uncertainties for the 3 equilibria in Paul Lake for the Cascade experiment (top row, standardized level of chlorophyll *a*) and enrichment experiment (bottom row, standardized level of phycocyanin). Vertical dashed lines show equilibria of the original data.

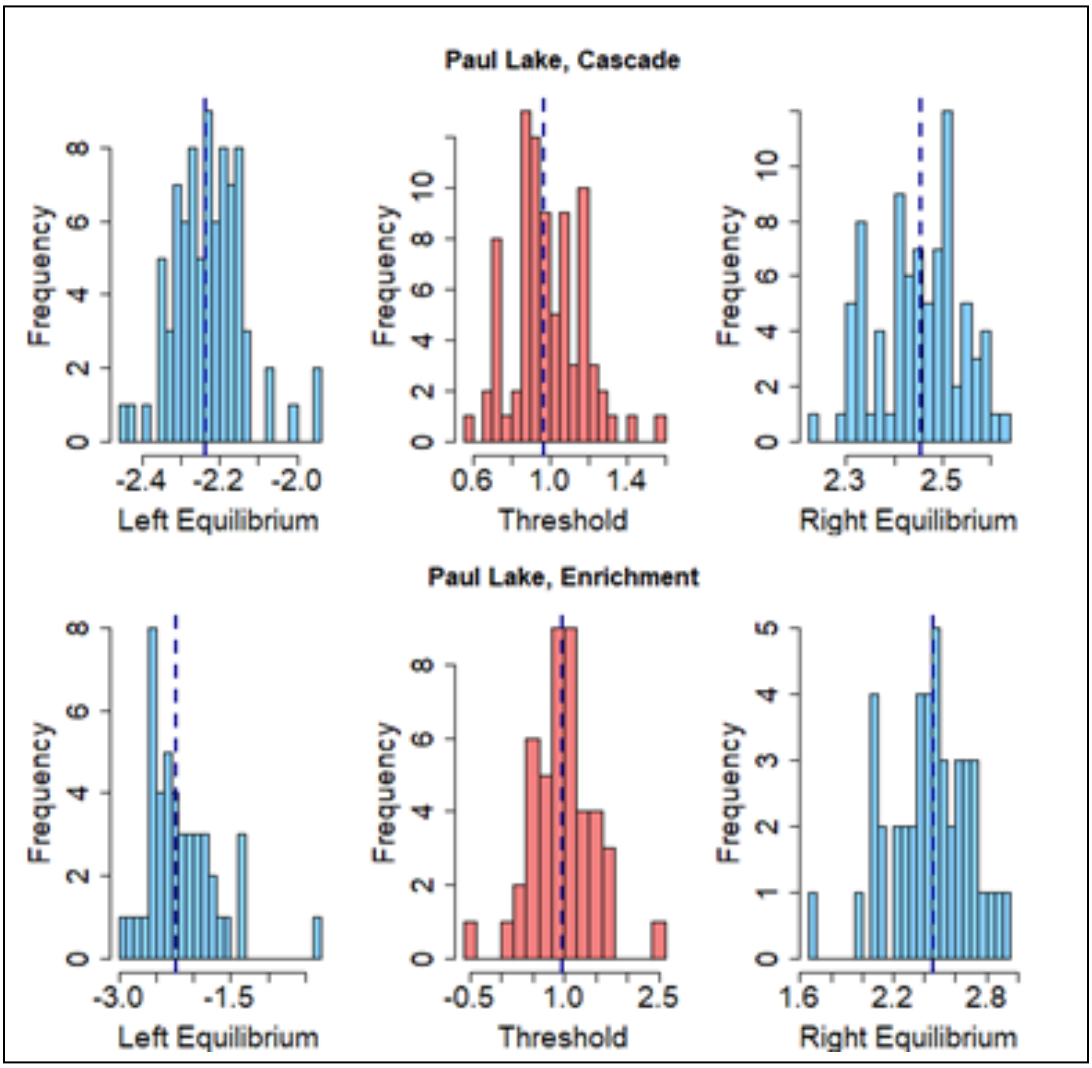

Bootstrapped Uncertainties for Exit Time

Figure S-8. Bootstrap estimates of uncertainty of exit time of Peter Lake for the Cascade (top row) and Eutrophication (bottom row) experiments, for the low-pigment (left column) and high-pigment (right column) basins observed in each experiment. Vertical dashed line shows the estimate from the original data.

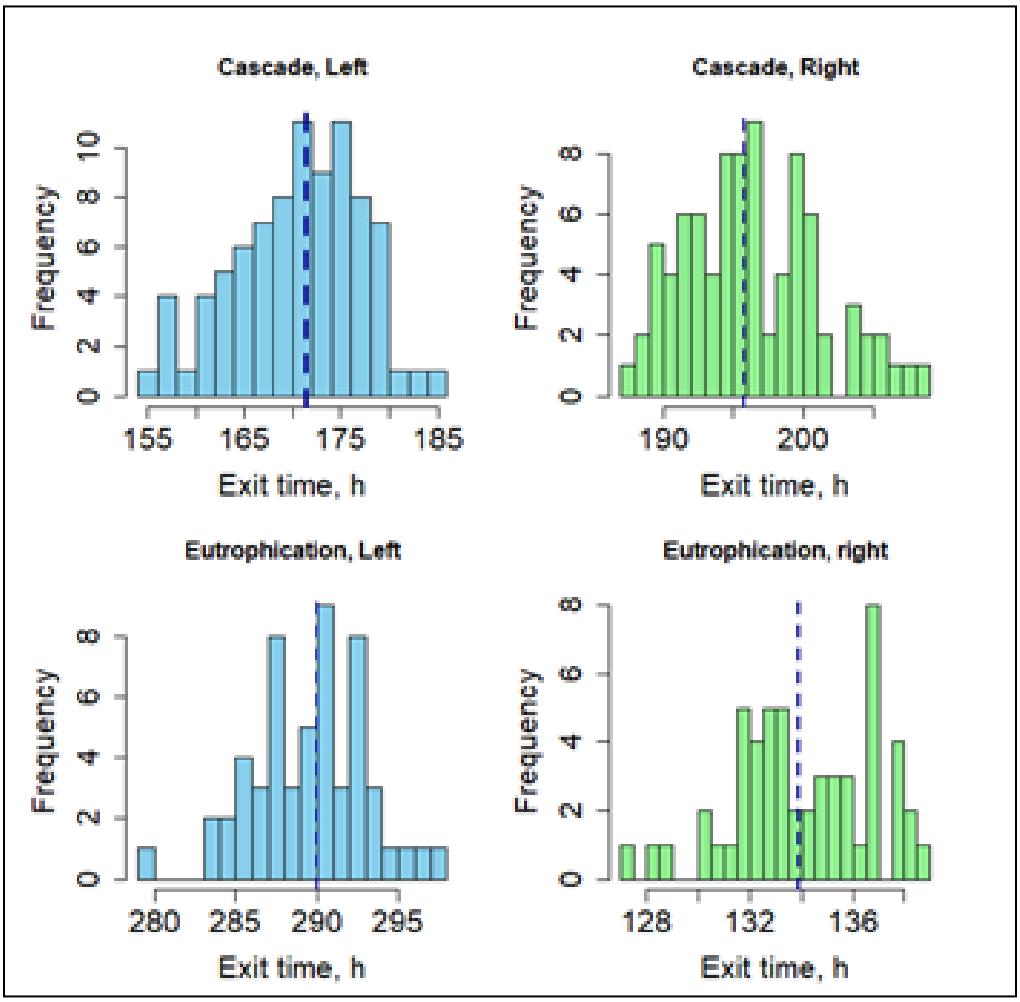

Figure S-9. Bootstrap estimates of uncertainty of exit time in the reference ecosystem, Paul Lake, for the Cascade (top row) and Eutrophication (bottom row) experiments, for the low-pigment (left column) and high-pigment (right column) basins observed in each experiment. Vertical dashed line shows the estimate from the original data.

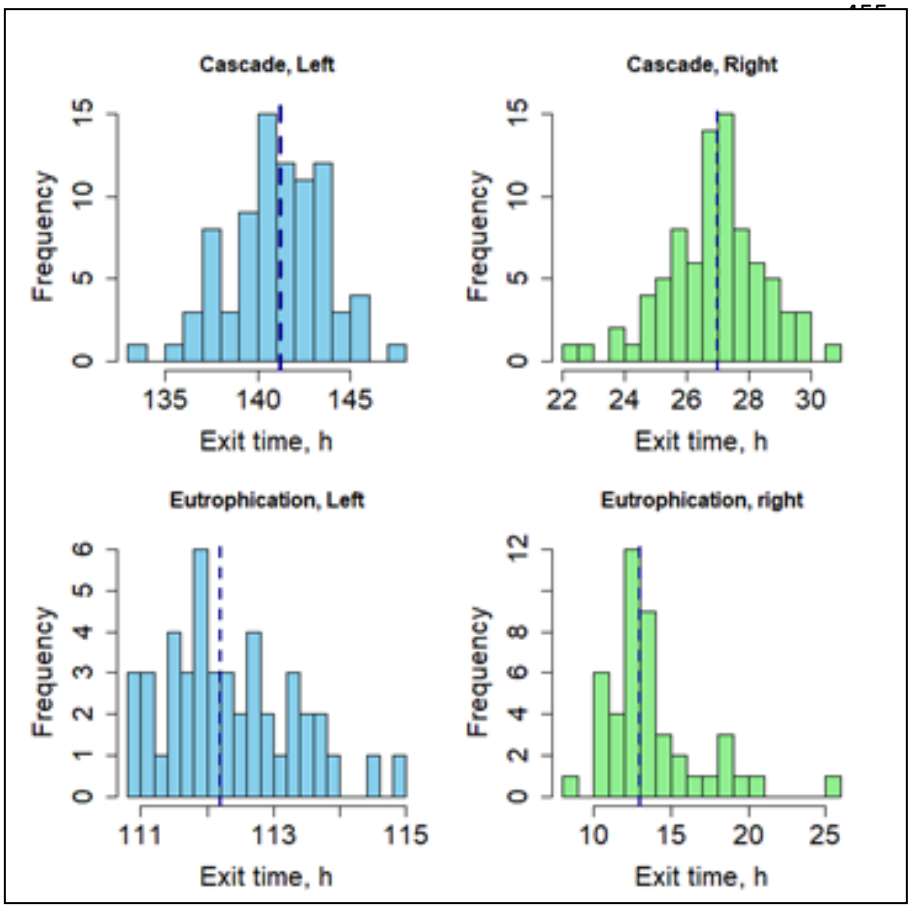

Could Alternate States be Detected by Chance?

We generated phase randomized surrogate time series to show whether we can get alternative stable states by chance. When our time series are randomized using the Ebisuzaki method using the surrogates() function in the R library "astrochron" we always get a model with a linear drift function D1 (implying one stable state) and additive noise (i.e. D2 has no apparent change or trend with state) (Figure S10). This is not useful for bootstrapped estimates of uncertainty of the mean exit time, but it does show that we are not likely to see alternate states by chance.

Figure S10. D1 and D2 from 100 pseudodata series from Peter Lake, Enrichment experiment, bootstrapped by the Ebisuzaki method. In each plot, solid line is the median of the 100 bootstraps for each state value and the dotted lines are the 10^{th} and 90^{th} quantiles.

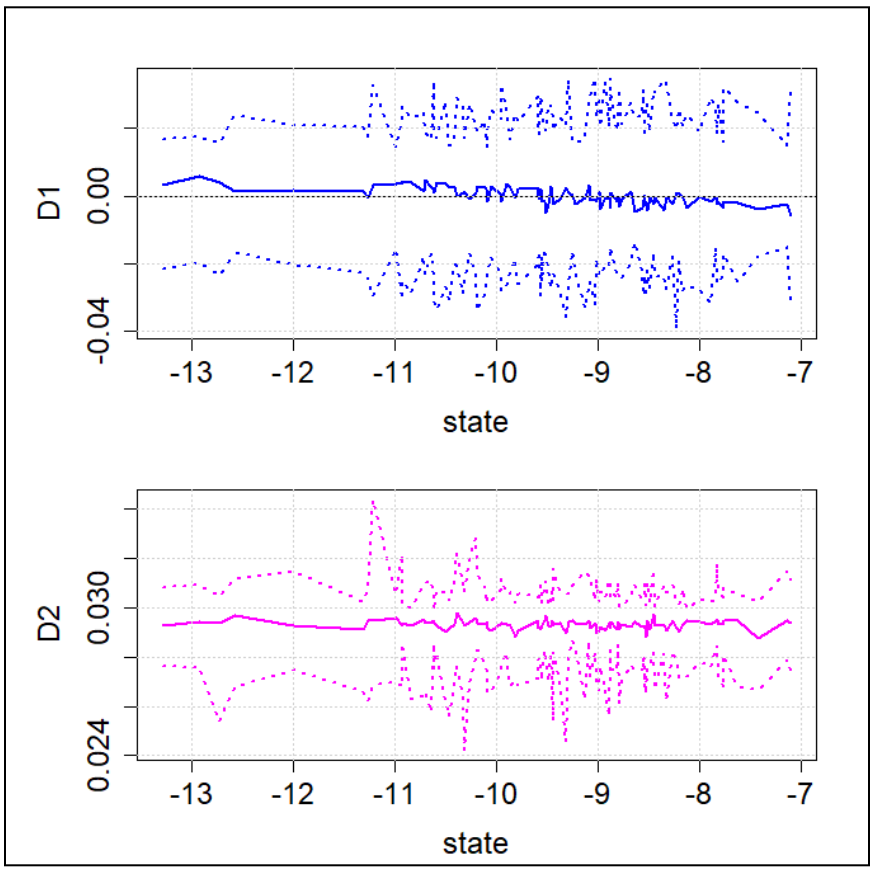

Alternate States in Daily Chlorophyll Time Series

We considered the possibility that alternate states in Paul Lake were related to variability of sonde data or events of short duration. To check this possibility we analyzed daily chlorophyll samples collected from both lakes on each day of the Cascade and Enrichment experiments. Chlorophyll sampling was conducted throughout the period of summer stratification each year. Water samples from a depth of 0.5 m were collected over the deepest point in the lake each day. During the enrichment experiment water was collected before nutrient additions. The water was filtered through Whatman 47 mm GF/F filters and extracts from the filters were analyzed fluorometrically for chlorophyll *a* concentration corrected for pheopigments (Holm-Hanson 1978).

Daily chlorophyll time series were fitted to time-varying autoregressions (eq. S-1) and the level time series b_t (chlorophyll *a* in µg/L) was used to estimate drift and diffusion. Because of the long time step (1 day) and small sample size (460 intervals), we did not test the effects of longer time lags.

Chlorophyll time series in Paul Lake have only one equilibrium, the single root of the drift function (Fig. S9). In the enrichment experiment, the drift function comes close to the zero line at high chlorophyll levels but does not cross the zero line.

Chlorophyll time series from both experiments in Peter Lake have three equilibria, indicating two alternate states separated by an unstable threshold (Fig. S10).

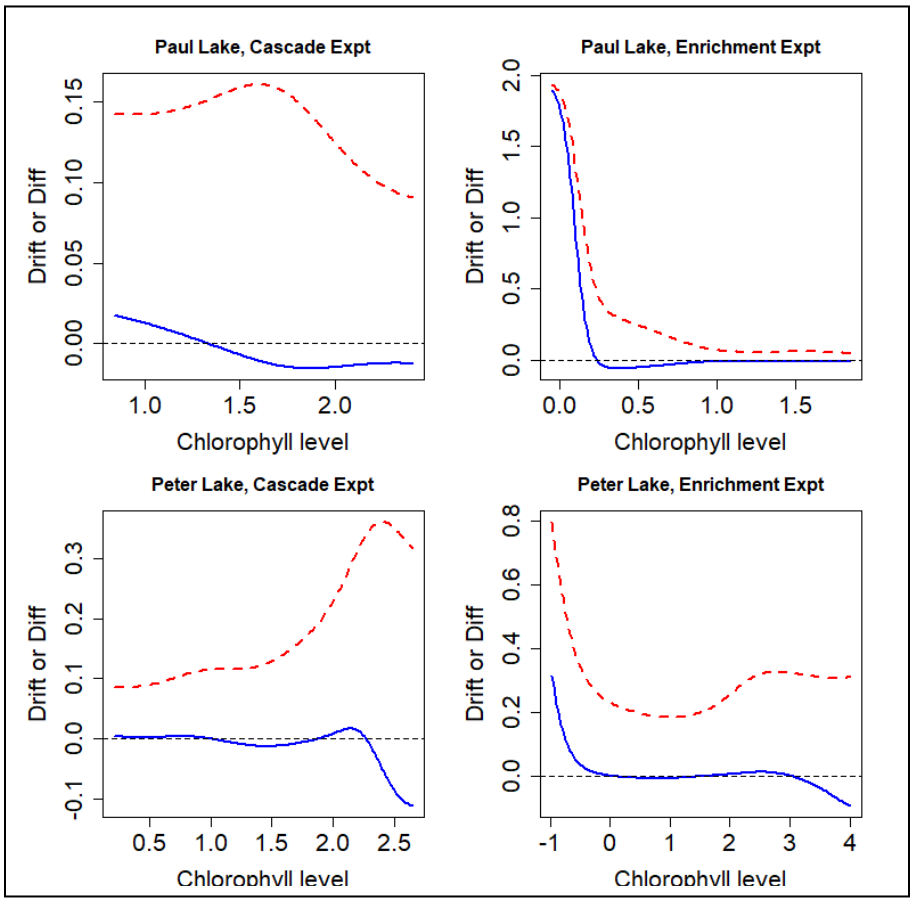

Figure S11. Drift (blue solid line) and diffusion (red dashed line) functions versus chlorophyll a level (µg/L) in Paul Lake, Cascade and Enrichment experiments. Dotted horizontal line at zero.

The daily datasets and metadata are available online:

Carpenter, S.R., M. Pace, J. Cole, J.F. Kitchell, and J. Hodgson. 2019. Cascade project at North Temperate Lakes LTER - Daily data for key variables in whole lake experiments on early warnings of critical transitions, Paul and Peter Lakes, 2008-2011 ver 1. Environmental Data Initiative. https://doi.org/10.6073/pasta/b0448233e215a969eb5623434fcd4494. Accessed 2021-01-01.

Pace, M., J. Cole, and S. Carpenter. 2020. Cascade project at North Temperate Lakes LTER - Daily Chlorophyll Data for Whole Lake Nutrient Additions 2013-2015 ver 2. Environmental Data Initiative. https://doi.org/10.6073/pasta/d480f53082da7ea53e349183a0c8a714. Accessed 2021-01-01.

References

Arani, B. M. S., S. R. Carpenter, L. Lahti, E. H. van Nes, and M. Scheffer. 2021b. Exit time as a measure of ecological resilience. Science **372:** eaay4895.

Carpenter, S. R., B. M. S. Arani, P. C. Hanson, M. Scheffer, E. H. Stanley, and E. Van Nes. 2020. Stochastic dynamics of Cyanobacteria in long-term high-frequency observations of a eutrophic lake. Limnology and Oceanography Letters **5:** 331-336.

Friedrich, R., J. Peinke, M. Sahimi, and M. Reza Rahimi Tabar. 2011. Approaching complexity by stochastic methods: From biological systems to turbulence. Physics Reports **506:** 87-162.

Hassanibesheli, F., N. Boers, and J. Kurths. 2020. Reconstructing complex system dynamics from time series: a method comparison. New Journal of Physics **22:** 073053.

Holm-Hanson, O. 1978. Chlorophyll a determination: improvements in methodology. Oikos **30:** 438-447.

Ives, A. R., and V. Dakos. 2012. Detecting dynamical changes in nonlinear time series using locally linear state-space models. Ecosphere **3:** art58.

May, R. M. 1977. Thresholds and breakpoints in ecosystems with a multiplicity of stable states. Nature **269:** 471-477.

Pole, A., M. West, and J. Harrison. 1994. Applied Bayesian forecasting and time series analysis. Chapman & Hall.

Tabar, M. R. R. 2019. Analysis and Data-Based Reconstruction of Complex Nonlinear Dynamical Systems. Springer Nature.

West, M., and P. J. Harrison. 1989. Bayesian Forecasting and Dynamic Models. Springer-Verlag.